Control System of the Reverse Electromechanical Scanner

VALENTIN DROZDOV
Department of Electrical Engineering and Precision Electromechanical Systems
ITMO University
197101, Saint-Petersburg, Kronverkskij Ave., 49
RUSSIAN FEDERATION
drozdovuprint@rambler.ru

VALENTIN TOMASOV
Department of Electrical Engineering and Precision Electromechanical Systems
ITMO University
197101, Saint-Petersburg, Kronverkskij Ave., 49
RUSSIAN FEDERATION
tomasov@ets.ifmo.ru

SERGEY TUSHEV
Department of Electrical Engineering and Precision Electromechanical Systems
ITMO University
197101, Saint-Petersburg, Kronverkskij Ave., 49
RUSSIAN FEDERATION
tushev.sergei@gmail.com

Abstract: The synthesis of controller algorithm for reversible electromechanical scanner of the telescope scanning axis is discussed. Digital control system is built without intermediate stage of synthesis of analog control law. The modified procedure for the synthesis of discrete optimal control law is introduced. This procedure involves the choice of quadratic functional penalty matrices to be replaced with the choice of system stability level. It is proved, that static control system of electromechanical scanner has better characteristics than first order astatism control system.

Key-words: electromechanical scanner, discrete control law, modified discrete optimal quadratic control.

1 Introduction

Nowadays terrestrial optical-electronic tools (according to tradition they are often called optical telescopes) play a major role in the detection and monitoring of space objects, especially at large distances. Undoubted and unique advantages of optical telescopes are the following:

- the ability to detect distant objects by the sun or laser illumination in the night or twilight sky,
- the ability to detect objects in the infrared wavelength range of their own thermal radiation,
- high precision determination of the angular coordinates of objects,
- possibility of obtaining optical images of space objects and high-precision photometric and spectrophotometric measurements of their optical brightness.

Telescope works at infrared wavelength range and is designed to scan space object. It is set to the mount to control the angular position of the optical axis in the space. As usually, a mount has three axes of rotation: azimuth, elevation and scanning. Scanning axis is often made in the form of electromechanical scanner. Development of these mounts and control systems for near space observation is one of the most difficult problems of modern precision instrument making. The fact is that the mount and electromechanical control systems, solving the problem of scanning an object observed, should provide unique high quality targeting. All the elements of the design concept and its mount play an important role for such problems. Usually, mount is represented as a two-mass

ISBN: 978-960-474-383-4

mechanism in the process of modeling and design of electric drives. The angular resonance frequency of the mechanism caused by the torsional deformation determines frequency bandwidth of the control system, and as a result, its performance [1-4].

2 Mathematical model of scanner

A mathematical model of the magnetic spring, which is used in the scanning axis of the telescope, has the following form

$$\begin{cases} \dfrac{di}{dt} = -\dfrac{R}{L} i - \dfrac{K_e}{L}\omega + \dfrac{1}{L}u \\ \dfrac{d\omega}{dt} = \dfrac{K_i}{J} i - \dfrac{K_\alpha}{J}\alpha - \dfrac{1}{J}M_c \\ \dfrac{d\alpha}{dt} = \omega \end{cases}, \quad (1)$$

where R is winding resistance, L is leakage inductance of the control winding, K_e is coefficient of back EMF, J is moment of inertia, f is coefficient of moment of viscous friction force, M_c is resistance torque, K_i is stiffness of speed-load curve or current sensitivity, K_α is stiffness of speed-load curve or current sensitivity or stiffness of magnetic spring. Typically, the viscous friction coefficient has a small value, so it might be neglected [5-7].

In the above equations u is control voltage, i is current in the control winding, α is rotation angle and ω is rotation speed. The most common case in practice is when current sensor and position sensor included in the control system.

Standard state-space model (1) is

$$\begin{aligned} \dot{x} &= A_g x + B_g u + B_{gc} M_c \\ y &= C_g x \end{aligned}, \quad (2)$$

where

$$A_g = \begin{bmatrix} -\dfrac{R}{L} & -\dfrac{K_e}{L} & 0 \\ \dfrac{K_i}{J} & 0 & -\dfrac{c_u}{J} \\ 0 & 1 & 0 \end{bmatrix}, B_g = \begin{bmatrix} \dfrac{1}{L} \\ 0 \\ 0 \end{bmatrix}, B_{gc} = \begin{bmatrix} 0 \\ -\dfrac{1}{J} \\ 0 \end{bmatrix},$$

$$C_g = \begin{bmatrix} 1 & 0 & 0 \\ 0 & 0 & 1 \end{bmatrix}.$$

Microprocessor implementation of the control system is a requirement now. The problem of synthesis algorithm controller directly, bypassing the stage of the synthesis of analog control law with its subsequent sampling, is relevant. In order to solve it, a differential system of equations is transformed into a system of difference equations (3).

$$\begin{aligned} x_{m+1} &= A_{dg} x_m + B_{dg} u_m + B_{dgc} M_{cm} \\ y_m &= C_{dg} x_m \end{aligned} \quad (3)$$

Nowadays mathematical package MATLAB is a powerful tool for design of control systems. By using this package, transformation from the model (1) to the model (2) with a sampling interval T_d is performed using a built-in command *c2d*. When synthesis of control algorithm is provided, moment of resistance M_c is neglected, but it is taken into account when modeling the control system.

The reference signal of electromechanical scanning system is a periodic signal consisting of working areas with forward and reverse and two reversing areas in each period. A typical graph of one period of reference signal is shown on Figure 1.

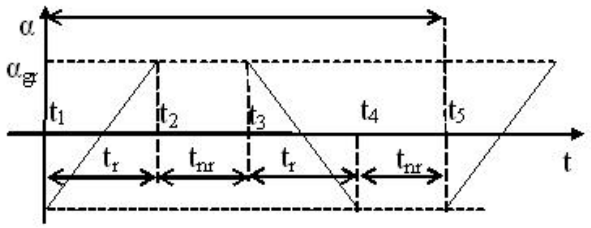

Figure 1. Reference signal in scanning system, t_r is time of working area, t_{nr} is time of non-working area.

According to Figure 1 a reference signal at the working area is changed at a constant speed. For zero steady-state position error control system requires to have second order astatism. Control object (1) is static, and second order astatism could only be achieved by adding two integrators (adders in the discrete version) in the control law. But the implementation of integrators leads to a significant overshoot in transient response. In this case, there are significant transient errors at the beginning of each working section after reversing the actuator.

3 Synthesis of controller

In a static system in the work area there is a constant speed error and linearly changing position error. However, it is possible that the absolute value of these errors will be much smaller than when integrators are included in the control law [8, 9].

It is necessary to synthesize linear-quadratic-Gaussian (LQG) discrete controller with first order observer, due to absence of speed sensor and without an integrator. In this case, a closed loop system is static. LQG controller provides the location of the state eigenvalues of a closed loop system within the circle of unit radius centered at the origin for any choice of positive definite penalty matrices. In addition, optimal control provides sufficiently large reserves stability which ensures smooth transient.

ISBN: 978-960-474-383-4

However, it is well known that there are no rules of proved choice of penalty matrices, it is often guided by brute force. It is necessary to provide transient time for continuous object (1), which is determined by the degree of stability η. Then the roots of the characteristic equation of a discrete system consisting of a discrete controller and the object (1), must lie within a circle centered at the origin of radius $r = e^{-\eta T}$. Auxiliary matrices are

$$A_n = \frac{A_{dg}}{r},\ B_n = \frac{B_{dg}}{r} \qquad (4)$$

If you select the positive η with appropriate dimension, then feedback matrix, which is obtained from the solution of the discrete Riccati equation, guarantees the location of the eigenvalues of the matrix (5) inside the circle of unit radius.

$$F_n = A_n - B_n K \qquad (5)$$

If expression (4) is substituted in (5), following expression could be obtained:

$$F_n = \frac{A_{dg}}{r} - \frac{B_{dg}}{r}K = \frac{1}{r}(A_{dg} - B_{dg}K) = \frac{1}{r}F\ .$$

And so, $F = rF_n$.

It is known that if matrices are associated by functional relation, the same is ratio of their eigenvalues. Hence the eigenvalues of F lie inside the circle of radius r.

As a result, only one number η is selected, which has a clear physical meaning and determining system performance, instead of selecting the penalty matrices by brute force.

$$u_m = -Kx_m \qquad (6)$$

Synthesized optimal control (6) cannot be implemented due to absence of the rotation speed sensor. As follows from (2) vector $y = \begin{bmatrix} i \\ \alpha \end{bmatrix}$ is measured. Missing information about the rotation speed can be obtained using low-dimensional observer. Expression (6) is transformed to

$$u_m = N_2 w_m + N_1 y_m \qquad (7)$$

where w_m is determined by solving the real-time difference equation $w_{m+1} = a_n w_m + b_n u_m + r_n y_m$.

The number a_n identifies a speed of estimation and is selected from the range $0 \le a_n < 1$.

Matrix r_n is chosen to provide controllability of pair (a_n, r_n), e.g., $r_n = [0\ 1]$. Coefficient b_n is determined by $b_n = T_n B_{dg}$, T_n is determined by solving Sylvester equation $a_n T_n - T_n A_{dg} + r_n C_{dg} = 0$. Matrices N_1 and N_2 in expression (7) are estimated like $\begin{bmatrix} N_1 & N_2 \end{bmatrix} = -K \begin{bmatrix} C_d \\ T_n \end{bmatrix}^{-1}$. The model of discrete controller is achieved:

$$\begin{aligned} w_{m+1} &= (a_n + b_n N_2) w_m + (b_n N_1 + r_n) y_m \\ u_m &= N_2 w_m + N_1 y_m \end{aligned}. \qquad (8)$$

The reference signal on Figure 1 should be generated so as to avoid shocks during the reverse of actuator and acceleration signal would be continuous. For this purpose, it is recommended triple integration of the third derivative of the reference signal. Its graph is shown in Figure 2, where $t_{z1} = \frac{t_{nr}}{2}$, $t_{z2} = \frac{t_{nr}}{2} + t_r$, $t_{z3} = t_{nr} + t_r$, $t_{z4} = \frac{3t_{nr}}{2} + t_r$, $t_{z5} = \frac{3t_{nr}}{2} + 2t_r$, $t_{z6} = 2(t_{nr} + t_r)$.

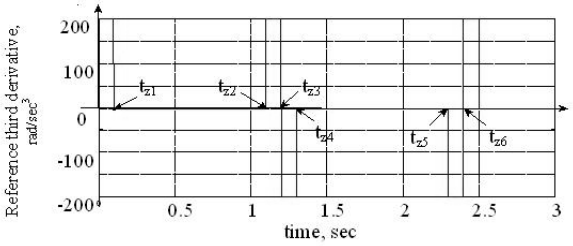

Figure 2. The third derivative of the reference signal.

The amplitude of the third derivative of the reference signal is calculated according to the formula

$$a_{max} = \frac{16\alpha_{gr}}{t_r t_{nr}^2}.$$

If $M_k = \frac{t_{zk}}{T}$, $k = 1,2,...,6$, then the flowchart of sequence generation algorithm, shown at Figure 2, is like on the upper part of Figure 3.

The state-space model of block of triple integration of analog setpoint has the form (9).

$$\begin{aligned} \dot{x} &= Ax + Bv \\ \alpha &= Cx \end{aligned} \qquad (9)$$

In (9)

$$A = \begin{bmatrix} 0 & 0 & 0 & 0 \\ 1 & 0 & 0 & 0 \\ 0 & 1 & 0 & 0 \\ 0 & 0 & 0 & -\frac{\beta}{T_s} \end{bmatrix}, B = \begin{bmatrix} 1 & 0 & 0 \\ 0 & 1 & 0 \\ 0 & 0 & 0 \\ 0 & 0 & -\frac{\beta}{T_s} \end{bmatrix},$$

$$v = \begin{bmatrix} a_3 \\ -c_1 \\ c_2 \end{bmatrix},\ C = \begin{bmatrix} 0 & 0 & 1 & 1 \end{bmatrix},$$

$$T_s = 2(t_{nr} + t_r),\ c_1 = \frac{8\alpha_{gr}}{t_r t_{nr}},\ c_2 = \alpha_{gr}\left(1 + \frac{2t_{nr}}{3t_r}\right).$$

Coefficient β in the setpoint model determines setting time of output periodic signal. The more time to establish oscillations, the smoother is the starting process of the scanning device. In case of the forced start autooscillations occur in the system

due to saturation of the power supply. It is often $3 \le \beta \le 6$.

Algorithm for generating discrete controller setpoint signal can be obtained from the expression (9), using the built-in MATLAB command *c2d*. Then the discrete state-space model of signal generator has the following form:

$$x_{m+1} = A_d x_m + B_d v_m .$$
$$\alpha = C_d x_m$$

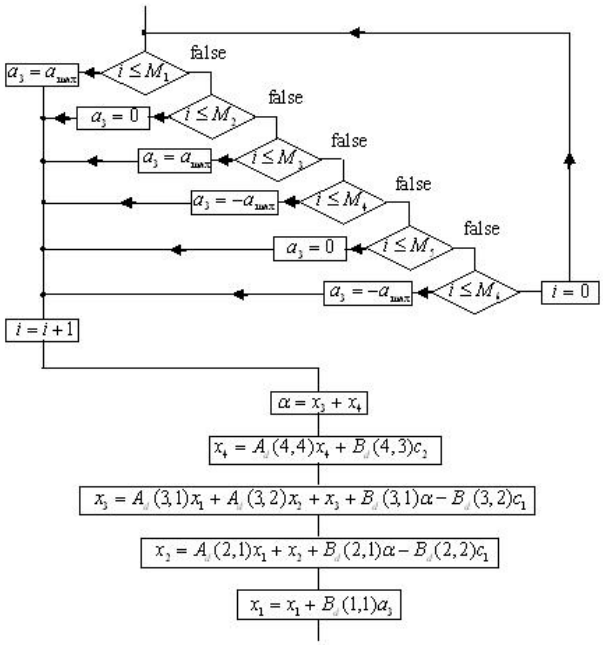

Figure 3. Flowchart of setpoint algorithm.

This model is used to construct an algorithm for generating reference signal with flowchart shown on Figure 3.

4 System modeling

Simulation scheme of a digital control system of electromechanical scanner is presented on Figure 4, where block *Subsystem 1*is model of discrete position setpoint, based on algorithm shown at Figure 3, block *Discrete State-Space* is discrete controller (8), block *Subsystem* is continuous object model (1).

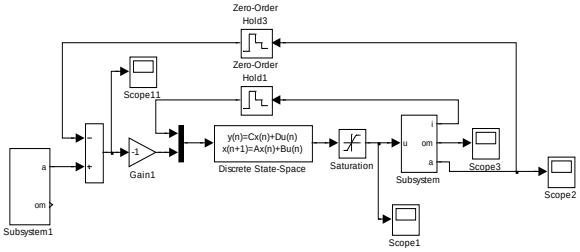

Figure 4. Simulation scheme of electromechanical scanner.

Modeling was provided for some concrete object with defined parameters. The output of electromechanical scanner system is shown at Figure 5.

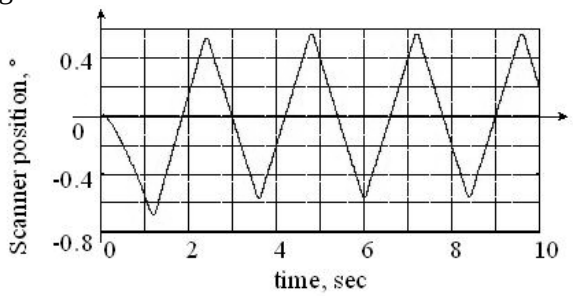

Figure 5. Scanner position signal.

Position error graph is shown at Figure 6. As can be seen from this figure position error at the work area does not exceed two percent. Speed error graph is shown at Figure 7. As can be seen from this figure steady speed error at the work area does not exceed two percent, too.

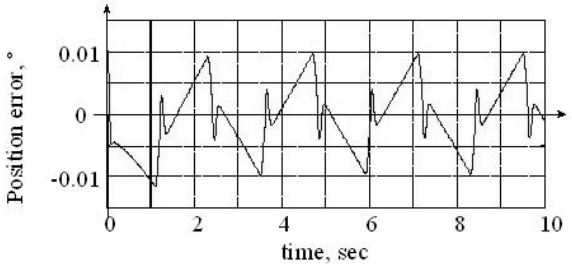

Figure 6. Scanner position error.

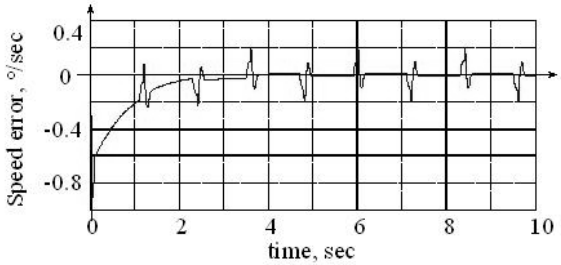

Figure 7. Scanner speed error.

The investigation of the system with a discrete controller, synthesized by the proposed method with first order astatism, showed the following results:

- steady-state speed error is zero at the working area,
- there is a significant short-term overshoot at the beginning of the working area, reaching 80%,
- constant position error at the working area is greater than 10%.

The above-mentioned results suggest that the static control system has better performance than

astatic first order and can be used to control the precision electromechanical scanner.

5 Conclusion

Digital controller synthesized using the intermediate stage of analog algorithm with its subsequent sampling, has the following drawback. Discretization of analog algorithms usually performed using a simple first-order Euler method, which does not guarantee high accuracy. Error of etimation of derivatives can accumulate when the control algorithm runs in real time and that leads to loss of stability of the system with the poor choice of the interval of discretization. Synthesis of a discrete algorithm with exception of intermediate continuous algorithm phase ensures system stability with any selected value of the sampling interval.

The advantage of the synthesis of optimal control is shown, when the procedure of selection of penalty matrices is replaced by choosing only one number characterizing the system performance. The results obtained are recommended for use in high-precision electric drives of precision observations complexes.

6 Acknowledgement

This work was financially supported by Government of Russian Federation, Grant 074-U01.

References:

[1] Sarhan, H.S. , Issa, R.H., Alia, M.A., Al-Abbas, I.K. Precision speed control of DC motor drive system, *International Review of Automatic Control*, Volume 5, Issue 5, September 2012, pp. 673-676.

[2] Balkovoi, A.P., Kostin, A.V., Myagkikh, A.S., Tolstykh, O.A., Tsatsenkin, V.K., Yakovlev, S.F. Design of direct linear drives for manufacturing, *Russian Electrical Engineering*, 2013, Vol 7(84), pp. 363-369.

[3] Drozdov V.N., Tushev S.A. Ship motions influence on the range of possible coordinates of object observed by telescope on the deck, *Vestnik IGJeU*, Ivanovo 2013, Volume 4, pp. 54-58

[4] Tomasov V.S., Lovlin S.Ju., Tushev S.A., Smirnov N.A. Output voltage distortion of pulse width converter of precision electric drive, *Ivanovo: Vestnik IGEU*, Vol. 1, 2013.

[5] Yu. P. Filyushov, V. Yu. Filyushov. Control of a synchronous machine under minimization of heat losses in conditions of minimal reactive power, *Russian Electrical Engineering*, December 2013, Volume 84, Issue 12, pp. 712-717.

[6] S. G. Voronin, D. A. Kurnosov, A. S. Kul'mukhametova. Vector control of permanent-magnet synchronous motors, Russian Electrical Engineering, October 2013, Volume 84, Issue 10, pp. 581-585.

[7] Worthington, M.S., Beets, T.A., Beno, J.H., Mock, J.R., Murphy, B.T., Southa, B.J., Good, J.M. Design and development of a high precision, high payload telescope dual drive system, *Proceedings of SPIE - The International Society for Optical Engineering*, Vol. 7733,, Issue PART 1, 2010.

[8] Ren, C., Liuzhao, Songlibin, Yiqiang, Chen, K., Zhang, Z. Design and simulation of the direct drive servo system, *Proceedings of SPIE - The International Society for Optical Engineering*, 2010.

[9] Tomasov V.S., Lovlin S.Ju., Tushev S.A., Smirnov N.A. Output voltage distortion of pulse width converter of precision electric drive, *Ivanovo: Vestnik IGEU*, Vol. 1, 2013.

[10] Sadovnikov Mikhail A., Tomasov Valentine S., Tolmachev Valery A., Precision Electric Drive for Optical Space Control Systems, *Scientific and Technical Journal «Priborostroenie»*, Vol. 54, No. 6, 2011, pp. 81-86

[11] Terec, R., Chindris, V., Szabo, L., Rafajdus. Position sensing system for switched reluctance motor control, *Proceedings of 9th International Conference, ELEKTRO 2012*, pp. 266-269.

[12] Chen, M.-Y. , Lu, J.-S. High-precision motion control for a linear permanent magnet iron core synchronous motor drive in position platform, *IEEE Transactions on Industrial Informatics* Volume 10, Issue 1, February 2014, Article number 6461410, pp. 99-108.

[13] Subbotin D.A., Lovlin S.Y., Tsvetkova M.H. Two-mass mathematical model of magnetoelectric converter for reversible scanning device // Manufacturing Engineering, Automatic Control and Robotics: Proceedings of the 14th International Conference on Robotics, Control and Manufacturing Technology (ROCOM '14) - 2014, No. 32/1/1, pp. 11-14

[14] Subbotin D.A., Lovlin S.Y., Tsvetkova M.H. Identifying dynamic model parameters of a servo drive // Manufacturing Engineering, Automatic Control and Robotics: Proceedings of the 14th International Conference on Robotics, Control and Manufacturing Technology (ROCOM '14) - 2014, No. 32/1/1, pp. 50-57